

Available online at [www.sciencedirect.com](http://www.sciencedirect.com)**ScienceDirect**

Procedia Engineering 99 (2015) 840 – 847

**Procedia  
Engineering**[www.elsevier.com/locate/procedia](http://www.elsevier.com/locate/procedia)

“APISAT2014”, 2014 Asia-Pacific International Symposium on Aerospace Technology,  
APISAT2014

# Performance Estimation for Differential Pressurization Pulse Jet Engine

Zhang Jianpeng, Qin Lizi\*, He Miaosheng

*School of Astronautics, Beihang University, Beijing 100191, China*

---

## Abstract

A novel differential pressurization pulse jet engine is suggested in this paper. Working process of the engine is firstly introduced, then several realistic assumptions are made, physical model and mathematical model of the engine's extrusion and filling process are built. Using Propane as fuel, the mathematical model can be solved by setting some parameters. Working characteristics of the engine in each stage are analysed, and performance parameters of the engine is estimated, such as pressure, thrust, and specific impulse. Through suitably changing several structure parameters, analysing the performance parameters, the impacts of structural parameters on the engine performance are discussed. Finally, compared with conventional pulse jet engines, this engine provides an approach to pressurize and has a higher ratio.

© 2015 The Authors. Published by Elsevier Ltd. This is an open access article under the CC BY-NC-ND license

(<http://creativecommons.org/licenses/by-nc-nd/4.0/>).

Peer-review under responsibility of Chinese Society of Aeronautics and Astronautics (CSAA)

**Keywords:** Movable injector, DPPJE, pressure ratio, structural parameters, performance;

---

## 1. Introduction

Pulse jet engine uses pulse combustion technology to produce intermittent thrust, it has a simple structure, low cost, and a high thrust to weight ratio, so it is highly valued in many countries, like America, Russia, and Japan. Pulse jet engine technique in Russia has been developed rapidly, especially in pulse jet engine with a small thrust. For a traditional pulse jet, it has some disadvantages, such as a low compression ratio, a low power and a small thrust. Refer to Christophe Koppel' compact pulse-rocket engine assembly, in ref. [1] and ref. [2], this paper

---

\* Corresponding author. Tel.: +86-10-82313789; fax: +86-10-82316855.

E-mail address: [qinlizi@126.com](mailto:qinlizi@126.com)

**Nomenclature**

$A$ Cross section area	$P$ Pressure
$l_p$ Displacement of injector	$v_p$ Velocity of injector
$\eta$ Relative discharge in injector	$\phi$ Relative discharge of nozzle exit
$\theta$ Temperature ratio	$f$ Friction on the injector
$\dot{m}$ Flow rate	$C_D$ Discharge coefficient
<b>Subscripts</b>	
$j$ Extrusion chamber	$c$ Combustion chamber
$b$ Inlet	$d$ Injection hole
$o$ Fuel injector	$e$ Nozzle exit

suggests a novel differential pressurization pulse jet engine (DPPJE), which has a movable injector in its internal. The DPPJE contains a movable injector---a differential area piston within a series of jet holes. The bulk of the DPPJE is divided into three parts: inlet, extrusion chamber and combustion chamber. The DPPJE has a spring in front of the movable injector, which can alleviate the velocity of the injector hitting the wall, and reduce staying time of the movable injector, structural diagram of the DPPJE is shown in Fig. 1.

When the engine starts, the movable injector overcomes friction and pressure of the combustion chamber, moves right, with pressure of the extrusion chamber and the inlet, elastic force of the spring acting on it. As the movable injector moving, air enters into the extrusion chamber through the intake port between the inlet and the injector. Meanwhile, fuel injector starts to spray fuel oil. Fuel oil enters into the extrusion chamber, mixes with air from the inlet and forms combustible mixture. When the movable injector reaches the limit stop, combustible mixture in the extrusion chamber enters into the combustion chamber through the injection holes. Once ignited, the combustible mixture begins to burn, pressure of the combustion chamber rises high and fuel gas rapidly exhausts from the convergent nozzle to produce thrust. The movable injector begins to move left since increasing pressure of the combustion chamber acting on it. Left side of the extrusion chamber has been completely closed and pressure of the extrusion chamber rises, the combustible mixture is squeezed into the combustion chamber. When the movable injector reaches the front wall, combustion mixture in the extrusion chamber has been completely ejected. With fuel gas in the combustion chamber exhausting, pressure of the combustion chamber drops. When pressure of the combustion chamber drops to a value, the movable injector moves right again, a new cycle begins. In this paper, working characteristics and performance of the DPPJE are theoretically analyzed, an approach to improve efficiency and increase thrust for conventional pulse jet engine is simultaneously provided.

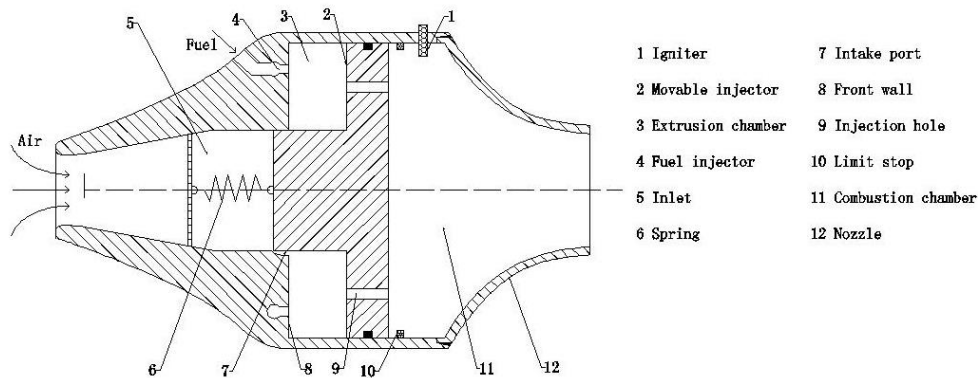


Fig. 1. Structural diagram of the DPPJE

## 2. Model

To analyze performance of the DPPJE, complex reactions in the combustion chamber is ignored in this paper, and following assumptions are established.

- (1) Mixture gas entering into the combustion chamber instantaneous finished combustion process and converted into fuel gas once ignited;
- (2) Gas in the combustion chamber and the extrusion chamber are both ideal gas, and uniformly distributed in the chambers;
- (3) Mixture gas's flow in injection holes can be described by a direct-flow injector flow equation;
- (4) Air is uniformly mixed with the fuel gas when it enters into the extrusion chamber;
- (5) Once the extrusion process finished, pressure of the extrusion chamber drops rapidly, till equal to pressure of the combustion chamber;
- (6) Flow in nozzle is a quasi-steady flow;
- (7) Friction of the movable injector in motion is regarded as a constant.

Assuming the flow is frictionless isentropic flow, zero-dimensional model is used in the extrusion chamber and the combustion chamber, 1-dimensional quasi steady model is used in nozzle. The model consists of equations on conservation of mass and energy in a control volume. A "lumped-parameter" or zero-dimensional formulation is used, in ref. [3]. Heat transfer is neglected. When the movable injector reaches the limit stop, the spring doesn't deform. While building the mathematic model, since the mixture of fuel gas atomized by fuel oil and air in the extrusion chamber, fuel oil is pulsed supplied. Based on motion equation of the injector and base conservation equation, adding gas equation of state and injection equation, mathematics model of the DPPJE is built as follow.

Analyzing the forces acting on the movable injector, the equation is

$$P_c(A_c - A_d) - P_b A_b - P_j(A_j - A_d) - f + K_s l_p = m_p \frac{dv_p}{dt} \quad (1)$$

$$dl_p / dt = v_p \quad (2)$$

Where  $P_c$  is pressure of the combustion chamber,  $P_b$  is pressure of the inlet,  $P_j$  is pressure of the extrusion chamber,  $f$  is friction force on the injector,  $K_s$  is elastic coefficient of the spring,  $l_p$  is the injector displacement from the origin,  $A_c$  is cross section area of the extrusion chamber,  $A_d$  is the whole cross section area of all the injection holes,  $A_b$  is cross area of the inlet,  $A_j$  is cross section area of the extrusion chamber,  $m_p$  is mass of the movable injector,  $v_p$  is the movable injector's velocity.

The instantaneous flow rate of mixed gas flow through the nozzle can be calculated as

$$\dot{m}_d = \begin{cases} \frac{C_D P_j A_d}{\sqrt{RT_j}} \sqrt{\frac{2k}{k-1} \left[ \left( \frac{P_c}{P_j} \right)^{\frac{2}{k}} - \left( \frac{P_c}{P_j} \right)^{\frac{k+1}{k}} \right]} & \text{when } \sigma_t < \frac{P_c}{P_{in}} < 1 \\ \frac{C_D P_j A_d}{\sqrt{RT_j}} \sqrt{2k \left( \frac{2}{k+1} \right)^{\frac{k+1}{k-1}}} & \text{when } \frac{P_c}{P_{in}} < \sigma_t \end{cases} \quad (3)$$

$$\eta = \frac{\int_0^t \dot{m}_d dt}{M} \quad (4)$$

Where  $\sigma_t = \left(\frac{2}{k+1}\right)^{\frac{k}{k-1}}$ ,  $C_D$  is flow coefficient,  $T_j$  is temperature of the extrusion chamber,  $M$  is total mass of fuel gas and air consumed in a pulse.

Assuming isentropic flow of ideal gas, the exiting mass flow is calculated from the choked flow expression.

$$\dot{m}_e = \Gamma(k) \frac{p_c}{\sqrt{R_c T_c}} q(\lambda_e) A_e \quad (5)$$

$$\phi = \frac{\int_0^t \dot{m}_e dt}{M} \quad (6)$$

Where  $T_c$  is instantaneous stagnation temperature in the combustion chamber, the exiting flow is assumed to be choked at all times, in ref. [4].

The mass conservation equation in the extrusion chamber and the combustion chamber are respectively

$$M_L - (V_{L0} - A_j l_p) \rho_j = M_L \eta \quad (7)$$

$$dm_c/dt = \dot{m}_d - \dot{m}_e \quad (8)$$

Where  $V_{L0}$  is the extrusion chamber's initial volume,  $\dot{m}_d$  is the flow rate of the injection holes.

The gas state equation in the extrusion chamber and the combustion chamber are respectively shown as

$$P_j = \rho_j R T_j \quad (9)$$

$$P_c (V_{c0} + A_c L_{p0} + A_c l_p) = m_c R_c T_c \quad (10)$$

Where  $\rho_j$  is density of the combustion mixture in the extrusion chamber.

According to the open cycle system first law of thermodynamics, energy equation of the extrusion chamber can be expressed as

$$d[c_v T_j \rho_j (V_{L0} - A_j l_p)] = -c_p T_j \dot{m}_d dt + P_j A_j v_p dt \quad (11)$$

Where  $c_v$  and  $c_p$  is respectively constant volume heat ratio and constant pressure heat ratio of mixture gas in the extrusion chamber.

Energy equation of the combustion chamber is also obtained.

$$\frac{d(\theta m_c)}{dt} = \dot{m}_d - k\theta \dot{m}_e - (k-1) \frac{p_c A_c v_p}{Hu} \quad (12)$$

Here  $\theta = \frac{T_c}{T_1}$ , it is the ratio of actual temperature of fuel gas and theoretical combustion temperature in combustion chamber,  $Hu = R_c T_1$ ,  $M_c$  is mass of the fuel gas in the combustion chamber.

When the movable injector reaches the front wall, the nozzle continues exhausting. Till  $p_c(A_c - A_d) + f - p_b A_b - p_j(A_r - A_d) - K_s L_p < 0$ , the movable injector starts to move right.

There are 12 unknown values in above 12 equations, which are  $v_p, p_j, p_c, m_c, \dot{m}_d, \eta, \dot{m}_e, \phi, l_p, \theta, \rho_d, T_j$ , the set of equations can be solved by using SIMULINK routing the classical Runge-Kutta method with a global error tolerance of  $1e-5$ .

When the movable injector starts to move right, the liquid gas is jet to extrusion chamber, the equation is

$$q_o = \mu A_o \sqrt{2 \rho_o (P_o - P_j)} \quad (13)$$

Where  $A_o$  is cross area of the fuel injector,  $\mu$  is flow coefficient of the fuel injector.

Energy equation, the mass conservation equation of the extrusion chamber should be changed. Engine's performance can be calculated using the model described above.

### 3. Results and discussion

In this section, some calculations are presented which show the effects of pulsed operation on performance. Propane and air is respectively utilized for fuel and oxidant, and they are mixed by a certain proportion. Structural parameter of the DPPJE is shown in Table1.

Table1. Structural parameters of the DPPJE

$A_c / m^2$	$A_j / m^2$	$A_b / m^2$	$A_e / m^2$	$A_d / m^2$	$L_d / m$	$L_p / m$
$2 \times 10^{-3}$	$1.2 \times 10^{-3}$	$0.8 \times 10^{-3}$	$2 \times 10^{-5}$	$5 \times 10^{-5}$	$5 \times 10^{-3}$	0.2

#### 3.1. Performance of the DPPJE

Three cycles after the engine starts are calculated. Since latter cycles are regular, the third cycle is chosen to study in detail.

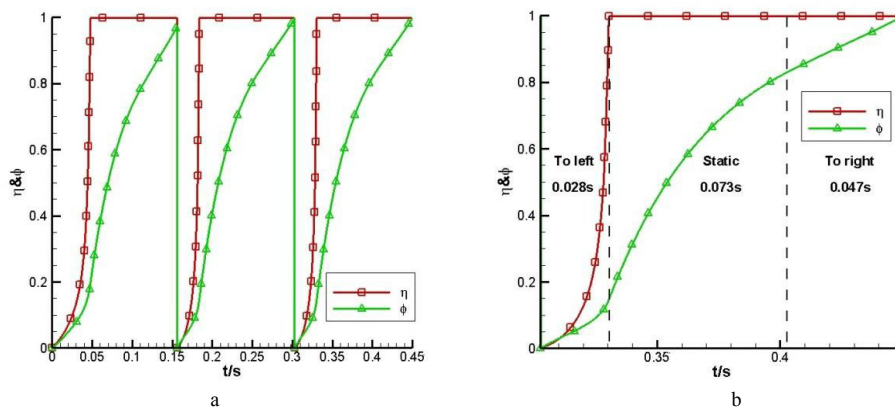


Fig. 2. (a) Discharges of the injector and the nozzle exit after the engine starts (b) Discharges of the injector and the nozzle exit in the third cycle

Fig. 2 shows relative discharges of the movable injector and the nozzle exit. We can observe working fluid's transfer when the engine is working. When the engine starts, with the movable injector moving left, combustion

mixture in the extrusion chamber enters into the combustion chamber, combustion gas generated in the combustion chamber begins to discharge. In Fig. 2a, relative flow curves of the three cycles are similar. When each cycle ends, the discharges are close to 1. While the movable injector reaches the limit stop, it immediately moved left without stopping. Discharge curves in the third cycle are shown in Fig. 2b. In the third cycle, when the injector reaches the front wall, 14.75% fuel gas has been discharged, most of the gas remains in the combustion chamber. When the injector starts to move right, 83.10% fuel gas has been discharged. From the figure, it is clear that the movable injector costs about 0.073s at a standstill in the front wall, approximately occupies half of the whole cycle.

The instantaneous pressures of the extrusion chamber and the combustion chamber are plotted in Fig. 3. As we can see, in the first cycle, peak pressures are relative low, ones in the latter cycles are higher, and keep little difference.

Now we observe the third cycle. In Fig. 3a, when the movable injector moves left, both of the pressures increase all the time. When the injector is close to the front wall, the pressures increase in intensity. The peak pressures appeared at the same time, the formers is 3.15MPa and the latter is 1.59MPa. Then they keep consistent according to the assumption (5). When fuel oil is ejected into the extrusion chamber, the pressure increases dramatically, till to 1.03MPa, and then it begins to drop sharply, always keeping higher than pressure of the combustion chamber. In figure 3b, the straight horizontal solid line denotes the average pressure of the combustion chamber, which is 0.4995MPa, and the dotted one denotes the average pressure of the extrusion chamber which is 0.5299MPa.

Temperature of the combustion chamber changes regularly when cycles are stable. If the injector moves left, it increases, else decreases.

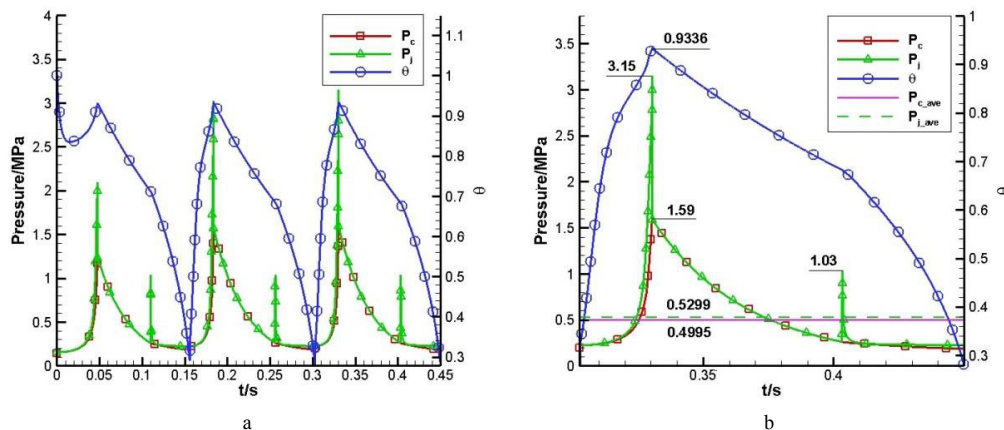


Fig. 3. (a) Pressures of the extrusion chamber and the combustion chamber, relative temperature after the engine starts (b) Pressures of the extrusion chamber and the combustion chamber, relative temperature in the third cycle

Instantaneous specific impulse and instantaneous thrust are calculated, as shown in Fig. 4. We can observe that instantaneous specific impulse changes similarly with temperature of the combustion chamber, and instantaneous thrust changes similarly with pressure of the combustion chamber. After the first cycle, they change periodically.

As we can see in the third cycle, thrust reaches the maxim value 60.22N, and specific impulse simultaneously reaches the maximum value 2177.4N/s. In Fig. 4b, the straight horizontal solid line denotes the average thrust in the combustion chamber, which is 18.9N, and the dotted one denoted the average specific impulse in the combustion chamber which is 1865.9N/s.

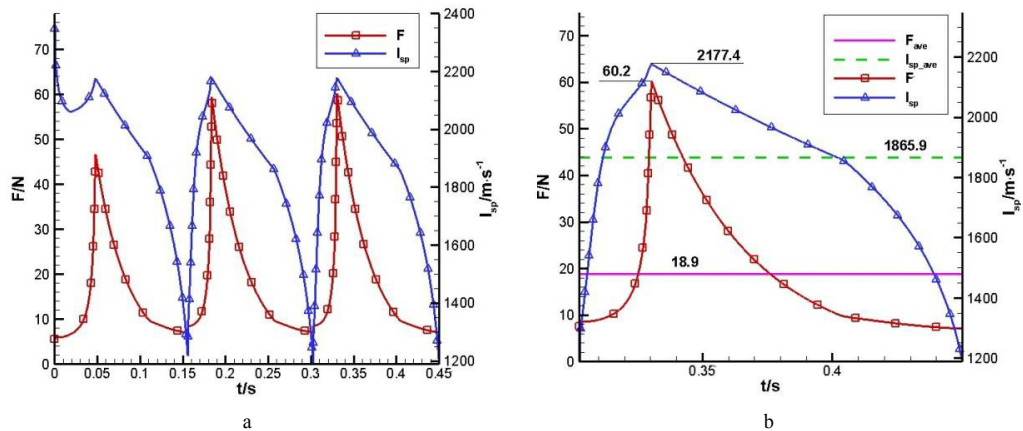


Fig. 4. (a) Thrust and specific impulse after the engine starts (b) Thrust and specific impulse in the third cycle

### 3.2. Influence of structural parameters

The above discussion shows the most important performance parameters of the DPPJE during its working process, especially in stable working cycles. The performance parameters of the DPPJE are calculated based on a set of constant structural parameters. Here, the influence of structural parameters for the DPPJE is researched. The third cycle is also chosen. Performance parameters in four cases are calculated. Case1 is the baseline, which is calculated in front. In case 2, area of nozzle exit is enlarged from  $2\text{e-}5\text{m}^2$  to  $3\text{e-}5\text{m}^2$ ; in case 3, cross area of the inlet is changed from  $0.8\text{e-}3\text{m}^2$  to  $1.0\text{e-}3\text{m}^2$ , meanwhile the cross section area of extrusion chamber is changed from  $1.2\text{e-}3\text{m}^2$  to  $1.0\text{e-}3\text{m}^2$ ; in case 4, maximum displacement of injector is lengthened from  $0.2\text{m}$  to  $0.3\text{m}$ , average pressures of the extrusion chamber and the combustion chamber, average thrust, and average specific impulse gotten under all cases above in the third cycle are shown in Table 2.

Table 2. Average performance parameters in different structural parameters

Cases	Case 1	Case 2	Case 3	Case 4
$A_e / \text{m}^2$	$2 \times 10^{-5}$	$3 \times 10^{-5}$	$2 \times 10^{-5}$	$2 \times 10^{-5}$
$A_j / \text{m}^2$	$1.2 \times 10^{-3}$	$1.2 \times 10^{-3}$	$1 \times 10^{-3}$	$1.2 \times 10^{-3}$
$A_b / \text{m}^2$	$0.8 \times 10^{-3}$	$0.8 \times 10^{-3}$	$1 \times 10^{-3}$	$0.8 \times 10^{-3}$
$L_p / \text{m}$	0.2	0.2	0.2	0.3
$P_{c\_ave} / \text{Pa}$	499521	351148	469190	574126
$P_{j\_ave} / \text{Pa}$	529932	377709	507545	613375
$F_{ave} / \text{N}$	18.89	19.92	17.74	21.71
$I_{sp\_ave} / \text{m} \cdot \text{s}^{-1}$	1866	1903	1863	1863

Through comparing case 1 and case 2, we found that, the larger area of the nozzle exit is, the lower pressures of the combustion chamber and the extrusion chamber are. Although the pressures drop, average thrust and average specific impulse increases, especially average specific impulse, is larger than 37. When area of the extrusion chamber reduces, it is clear see that the four parameters all decrease. When length of the combustion chamber increases from  $0.2\text{m}$  to  $0.3\text{m}$ , the average specific impulse is almost unchanged, but the pressures and the average thrust both increases. Certainly, with length of the combustion chamber increasing, consumption of fuel in a period increases. And a period of time approximately increases from  $0.15\text{s}$  to  $0.20\text{s}$ .

### 3.3. Advantages of the DPPJE

In order to demonstrate advantages of this DPPJE, pressure ratio of the DPPJE in the third cycle is compared with traditional pulse jet engines. Argus V1 engine, a pulse jet engine in ref. [5], has a pressure ratio of 1.94, and the pressure of combustion chamber is about 0.12Mpa. For this DPPJE, it can increase pressure of the combustion chamber to near 0.5Mpa, even higher. By comparison, the DPPJE has a larger pressure ratio. For a 50cm BMS engine in ref. [5], it has a theoretical thrust of 21N, and a test thrust of 25N. This DPPJE has a thrust around 20N, but a small size.

Through comparison, average pressure of combustion chamber of the DPPJE is obviously higher than one of normal pulse jet engine, pressure ratio of the DPPJE is also much higher. The novel pulse jet engine is valuable.

With these estimations we can consider some of the implications for practical applications, like performance improvement of engines with a small thrust.

### 4. Conclusions

A novel pulse jet engine is suggested in this paper, based on several assumptions, a relatively simple mathematics model of the engine's working process is built and presented. Through computing the model, performance of the DPPJE has been demonstrated. According to the movement of the injector, working process of the DPPJE can be distributed into three stages: to left, static, to right.

Though changing structural parameters, we found performance of the DPPJE is obviously influenced by structural parameters, such as area of the nozzle exit, length of the combustion chamber, etc. To obtain a better performance of this engine, the selection of structural parameters is critical.

Pressure ratio of the DPPJE is higher than conventional pulse jet engine, beyond 4. This type pulse jet engine has a simple structure, small size and higher pressure ratio, it is valuable to research. This DPPJE also provides a feasible reference to current and future engine design for requirement of small thrust.

### Acknowledgements

This work was supported by National Nature Science Foundation of China, No. 50706003.

### References

- [1] Christophe Koppel and Laurent Maine. Pulse Rocket Engine. United States: 5797260, Aug. 25, 1998
- [2] Christophe Koppel and Laurent Maine. Pulse Rocket Engine. United States: 5941062, Aug. 24, 1999
- [3] Qin L. Z., Liang S. Q., et al. A Novel Pulse Rocket Engine for Space Propulsion. AIAA 2009-5487
- [4] Edward B. Coy. Pulse Combustion Rockets for Space Propulsion Applications. AIAA 2003-1174
- [5] Wei T., Wu X. S., et al. Simplified analytical models for performance prediction of valveless pulse jet. Journal of Aerospace Power. 2012, 27 (1)